Received: 30 January 2020 | Revised: 10 March 2020 | Accepted: 2 April 2020

DOI: 10.1096/fj.202000131R

RESEARCH ARTICLE

THE FASEB JOURNAL

Cell division cycle 23 is required for mouse oocyte meiotic maturation

Qian Zhou[1,2] | Jian Li[1,3] | Wei Yue[1,2] | Ang Li[1] | Tie-Gang Meng[1] | Wen-Long Lei[1,2] | Li-Hua Fan[1,2] | Ying-Chun Ouyang[1] | Heide Schatten[4] | Zhen-Bo Wang[1,2] | Qing-Yuan Sun[1,2]

[1]State Key Laboratory of Stem Cell and Reproductive Biology, Institute of Zoology, Chinese Academy of Sciences, Beijing, China

[2]University of Chinese Academy of Sciences, Beijing, China

[3]Department of Reproductive Medicine, Peking University Shenzhen Hospital, Shenzhen Peking University-The Hong Kong University of Science and Technology Medical Center, Shenzhen, China

[4]Department of Veterinary Pathobiology, University of Missouri, Columbia, MO, USA

Correspondence
Qing-Yuan Sun and Zhen-Bo Wang, State Key Laboratory of Stem Cell and Reproductive Biology, Institute of Zoology, Chinese Academy of Sciences, Beijing 100101, China
Email: sunqy@ioz.ac.cn (Q.-Y. S.) and wangzb@ioz.ac.cn (Z.-B. W.)

Funding information
This work was supported by the National Natural Science Foundation of China (31530049, 31871504, 31601201).

Abstract

Precise regulation of chromosome segregation during oocyte meiosis is of vital importance to mammalian reproduction. Anaphase promoting complex/cyclosome (APC/C) is reported to play an important role in metaphase-to-anaphase transition. Here we report that cell division cycle 23 (Cdc23, also known as APC8) plays a critical role in regulating the oocyte chromosome separation. Cdc23 localized on the meiotic spindle, and microinjection of Cdc23 siRNA caused decreased ratios of metaphase-to-anaphase transition. Loss of Cdc23 resulted in abnormal spindles, misaligned chromosomes, errors of homologous chromosome segregation, and production of aneuploid oocytes. Further study showed that inactivation of spindle assembly checkpoint and degradation of Cyclin B1 and securin were disturbed after Cdc23 knockdown. Furthermore, we found that inhibiting spindle assembly checkpoint protein Msp1 partly rescued the decreased polar body extrusion and reduced the accumulation of securin in Cdc23 knockdown oocytes. Taken together, our data demonstrate that Cdc23 is required for the chromosome segregation through regulating the spindle assembly checkpoint activity, and cyclin B1 and securin degradation in meiotic mouse oocytes.

KEYWORDS

aneuploidy, Cdc23, chromosome, meiosis, oocyte

1 | INTRODUCTION

Mammalian oocytes are arrested at prophase of first meiosis for a long time until a preovulatory surge of LH induces meiosis resumption of fully grown oocytes, as indicated by germinal vesicle breakdown, followed by the first meiotic spindle formation, homologous chromosome alignment, and first polar body extrusion.[1] Precise regulation of meiotic progression is important for the production of healthy oocytes.

Anaphase promoting complex/cyclosome (APC/C) is a large complex containing 11-13 subunit proteins. As a highly conserved E3 ubiquitin protein ligase, APC/C is reported to play critical functions in the regulation of metaphase/anaphase

Abbreviations: APC/C, anaphase promoting complex/cyclosome; Cdc23, cell division cycle 23; GVBD, germinal vesicle breakdown; IBMX, 3-isobutyl-1-methylxanthine; LH, luteotropic hormone; MTOC, microtubule organizing center; SAC, spindle assembly checkpoint; TPR, tetratricopeptide repeat.

© 2020 Federation of American Societies for Experimental Biology

transition in different organisms.[2-4] Before entering anaphase, cyclin B1 and securin are rapidly degraded, a process mediated by APC. APC is activated by Cdc20 at the anaphase onset, and it is activated by Cdh1 at the end of anaphase and G1/S stage.[5-7] Cyclin B1 degradation leads to reduction of Cdk1 activity and degradation of securin, which subsequently activates separase which cleaves cohesin to induce the separation of chromosomes in mitosis.[8] However, in the process of first meiosis, activated separase hydrolyzes the phosphorylated Rec8 subunit on the chromosome arms of bivalents and resolves chiasmata in metaphase/anaphase transition, generating dyad chromosomes containing two chromatids, which contain centromeres tied together by separase-resistant cohesion.[9] In the meiosis II stage, separase cleaves centromeric cohesin, leading to sister chromatids segregation, which resembles the process of mitosis.[10] Taken together, APC/C regulates the accurate chromosome segregation in both mitosis and meiosis. APC/C ensures the accuracy of the transition from metaphase to anaphase, by targeting specific mitotic regulators for proteolysis at distinct times during mitosis.[11] Previous study identified 20 subunits of APC/C, and these subunits can be divided into four categories according to the structure: substrate recognition module including CDC20 and CDH1; tetratricopeptide repeat (TPR) subunits containing cell division cycle 23 (Cdc23); catalytic module and the scaffold module.[12,13] TPR proteins are reported to regulate cyclin B proteolysis in yeast,[14] and ablation of Cdc23 inactivates APC, causing significantly mitigated cyclin B degradation in mammalian cells.[15]

Cdc23 was identified as a conserved subunit of APC/C,[16] and researchers have found that it is required for the completion of nuclear division in *Saccharomyces cerevisiae*.[17] Previous report showed that mutant Cdc23 *S cerevisiae* represented a metaphase-like arrest phenotype, with a large number of microtubules emanating from either pole and ending close to the center of the spindle.[18] In addition, mutation of Cdc23 in yeast also showed defects in both entering and exiting anaphase,[19] suggesting that Cdc23 may play an important role in at least two stages of the cell cycle, metaphase-to-anaphase transition and telophase-to-G1 transition. Other researchers found that Cdc23 participated in the process of DNA replication in cell proliferation, providing evidence for the diverse functions of Cdc23.[20-22]

In recent, AtAPC8, the homologous of Cdc23 in *Arabidopsis*, was reported to be required for male meiosis.[23] However, the role of Cdc23 during the mammalian oocyte meiosis remains unknown. Considering the gender differences in meiosis, whether and how Cdc23 regulates the female germ cell meiosis is worth studying. Therefore, we utilized the RNA interference to knockdown Cdc23 in mouse oocytes to study the function of Cdc23 during meiotic progression.

Here we found that mouse Cdc23 plays critical roles in oocyte meiotic maturation. Loss of Cdc23 causes reduced first polar body extrusion by inducing abnormal spindles and misalignment of chromosomes. Further analyses showed delayed SAC inactivation, failed cyclin B1 and securin degradation, and disturbed chromosome segregation in oocytes lacking Cdc23. Further, inhibition of Mps1, a spindle assembly checkpoint kinase, not only increased the ratio of first polar body extrusion, but also reduced the expression level of securin in Cdc23 siRNA injected oocytes. These results suggest a critical role for Cdc23 in the regulation of mammalian oocyte meiotic maturation.

2 | MATERIALS AND METHODS

2.1 | Ethics statement

All experiments and methods referred to in this study were conducted under the guidelines of the Ethics and Experimental Animal Committee of the Institute of Zoology, Chinese Academy of Sciences, China.

2.2 | Oocyte collection, microinjection, and culture

The GV oocytes were collected from 8-week-old female ICR mice. Female mice were intraperitoneally injected with 5 IU PMSG to promote follicular maturation, and 48 hours later, mice were sacrificed for oocyte collection. The ovaries were dissected and then chopped with a razor blade. Tissue fragments were suspended with prewarmed (37°C) M2 medium (Sigma) supplemented with 200 μM IBMX to prevent GVBD. The GV oocytes were pick out using a prefabricated glass tube. In order to collect oocytes at different meiotic stages, the GV oocytes were washed three times in IBMX-free M2 medium, and transferred into pre-warmed microdrops containing M16 medium in a condition of 37°C, 5% CO_2. At 0, 4, 8, and 12 hours after the incubation, oocytes at the GV, GVBD, MI, and MII stages were collected. siRNAs were synthesized by the Gene Pharms (Suzhou, China). A concentration of 10 mM siRNA was injected into the GV oocyte cytoplasm in M2 medium containing IBMX. Control siRNA (5′-UUUUCCGAACGUGUCACGUTT-3′; 5′-ACGUGACACGUUCGGAGAATT-3′) was used as negative control. Cdc23 siRNA (5′-CAUGCUGUGUAAUUG GCAATT-3′; 5′-GGCCUACUUUGAUGUUAAATT-3′) was used to knock down the Cdc23. During the culture process, oocytes were transferred in pre-balanced M16 medium microdrops at 37°C in an atmosphere of 5% CO2 for specific time periods during further culture.

2.3 | mRNA extraction and quantitative real time-PCR

Total oocyte RNA was extracted from oocytes using RNeasy Mini Kit (Qiagen, Hilden, Germany) following the manufacturer's instructions. The mRNA level of each gene was

validated by quantitative real-time PCR (qRT-PCR) analysis on Light Cycler® 480 (Roche, Switzerland) according to the manufacturer's instructions.

2.4 | Immunofluorescence and confocal microscopy

Oocytes were fixed in 4% paraformaldehyde (PFA) in phosphate-buffered saline (PBS, pH 7.4) for 30 minutes at 37°C. After being permeabilized with 0.5% Triton X-100 for 30 minutes at room temperature, oocytes were blocked in 1% bovine serum albumin (BSA)—supplemented with PBS (pH 7.4) at room temperature for 1 hour and incubated overnight at 4°C with 1:1000 diluted primary antibody. After three washes in wash buffer (PBS containing 0.1% Tween-20 and 0.01% Triton X-100), the oocytes were incubated with corresponding F594 or F488-conjugated secondary antibody at room temperature for 1 hour. Oocytes were stained with 1:10 000 diluted 4′,6-diamidino-2-phenylindole (DAPI, 10 μg/mL in PBS) for 20 minutes. Then, the oocytes were mounted on glass slides and examined with a confocal laser scanning microscope (Zeiss LSM 780, Carl Zeiss AG, Germany). Images were processed using ZEN imaging software (Blue edition) and quantified using ImageJ software. To minimize the batch effect, all images were taken in the same environment using the same parameters.

2.5 | Chromosome spread

Oocytes were incubated in Tyrode's solution (Sigma, T1788) for 1 minute to remove the zona pellucida. After washing for three times in M2 medium, oocytes were transferred to the glass slide for breaking and fixing. A 0.5 cm × 0.5 cm rectangle frame was drawn on the glass slide with a hydrophobic pen. The breaking and fixing buffer was prepared as methanol: glacial acetic acid (3:1). After adding 20 μL breaking and fixing buffer, oocytes were moved into the liquid drop, and incubated overnight at 4°C. The following steps are the same as immunofluorescent staining. Bub3 and Mad2 antibody (1:1000) were incubated overnight at 4°C. Hoechst 33342 or PI was used to stain the chromosomes.

2.6 | Cdc23 and Cyclin B1 expression plasmid construction and mRNA microinjection

Total RNA extracted from mouse GV oocytes were utilized to synthesize the first strand cDNA using the cDNA synthesize kit (Abm, G490). The CDS region was amplified by PCR and cloned to pcDNA3.1(+)-Venus plasmid using Hieff clone one step cloning kit (Yeasen, 10905ES25). The linearized fusion plasmid was utilized as template for the production of capped mRNA by mMESSAGE mMACHINE Sp6 kit (Ambion). Poly (A) tail was synthesized by Poly (A) Polymerase Tailing Kit (Lucigen). Finally, mRNA was purified by RNeasy cleanup kit (Qiagen) for microinjection and further immunofluorescence staining. Cyclin B1-EGFP mRNA was produced in the same way.

2.7 | Time-lapse live-cell imaging

The GV oocytes were injected with 10 pL of 20 ng/μL Cyclin B1-EGFP mRNA in M2 medium containing 200 μM IBMX and cultured for 2-3 hours to allow Cyclin B1-EGFP expression. Oocytes were cultured in IBMX-free M16 medium in a European Molecular Biology Laboratory microscope incubator (GP106) during imaging. Time-lapse live-cell imaging was performed using Zeiss LSM510 META confocal microscope with an exposure time ranging from 200-500 ms depending on the fluorescence level. The acquisition of images was controlled by Volocity software.

2.8 | Western blotting

For western blot analysis, 200 oocytes were used for each group. The antibodies used were anti-CCNB1 (ab181593, abcam, 1:2000), anti-Securin (ab26273, abcam, 1:2000), anti-CDC23 (AF2716, Beyotime, 1:2000), anti-β-actin antibody (TA-09, Zhongshanjinqiao, 1:2000). Signals were captured with the ChemiDoc Imaging Systems (BioRad).

2.9 | Statistical analysis

Statistical analysis and significance, and n value are reported in the figure legends. Statistical analysis was conducted using Prism 7 (GraphPad). Differences between two groups were compared using Student's *t* test unless specified. A value of $P < .05$ was considered to be significant, and $P > .05$ was considered to be not significant.

3 | RESULTS

3.1 | Expression and subcellular localization of Cdc23 during mouse oocyte meiotic maturation

To investigate the function of Cdc23 during mouse oocyte meiotic progression, we examined the Cdc23 expression. Oocytes at different meiotic stages were harvested for western blot analysis. As shown in Figure 1A, Cdc23 was expressed

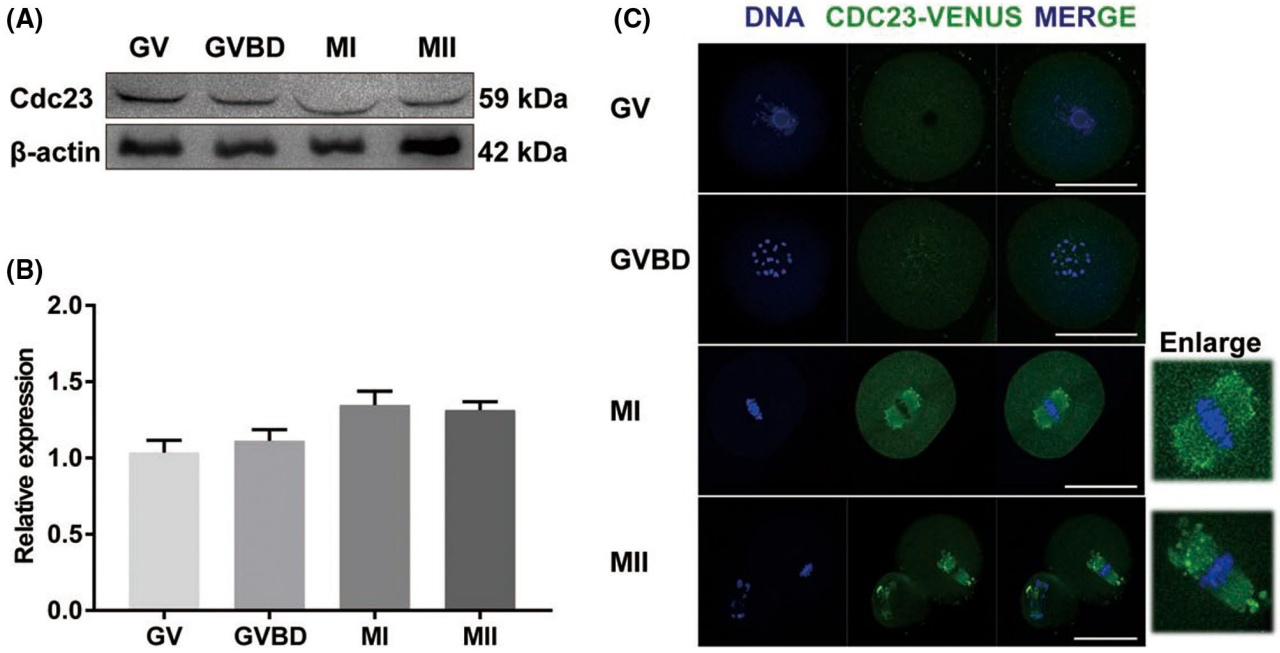

FIGURE 1 Expression and subcellular localization of Cdc23 during mouse oocyte meiotic maturation. A, Expression level of Cdc23 identified by Western blotting. A total of 200 GV oocytes were collected after culture for 0, 4, 8, and 12 hours in IBMX-free M16 medium, corresponding to meiotic stages of germinal vesicle (GV), germinal vesicle breakdown (GVBD), metaphase I (MI) and metaphase II (MII), respectively. B, Relative expression of Cdc23 during oocyte meiotic maturation. C, Subcellular localization of Cdc23 as revealed by CDC23-Venus mRNA injection and confocal microscopy imaging. Oocytes were microinjected with 100 ng/μL in vitro-transcribed Cdc23-Venus mRNA and cultured in M16 medium containing 200 μM IBMX for 4 hours, and released in IBMX-free M16 medium for further culture. At the corresponding meiotic maturation stages, oocytes were fixed and stained with Hoechst 33342 to visualize DNA (blue). Scale bar = 50 μm

during all stages of meiotic maturation, including GV, GVBD, MI, and MII stages, and the intensity of Cdc23 expression level was stable (Figure 1B). To study the subcellular specific distribution of Cdc23, we constructed *pCdc23-Venus* plasmid to synthesize Cdc23-Venus mRNA, and the in vitro transcribed mRNA was microinjected into the cytoplasm of mouse oocytes. As shown in Figure 1C, Venus-tagged Cdc23 did not show clear subcellular localization during the GV and GVBD stages. However, in MI and MII stage oocytes, Cdc23 was mainly localized at the spindle region, with a strong co-localization signal with alpha-tubulin. In addition, Cdc23-venus also located at MTOCs (microtubule organizing center), as indicated by the intense localization signal at spindle poles.

3.2 | Cdc23 depletion does not affect GVBD, but causes reduced PB1 extrusion

To gain insight into the role of Cdc23 in regulating mouse oocyte maturation, we inhibited the synthesis of Cdc23 by knocking down mouse Cdc23 through RNA interference. Cdc23-specific siRNA or scrambled siRNA was microinjected in the cytoplasm of GV stage oocytes. After inhibition in M2 medium containing 200 μM IBMX for 24 hours, the oocytes were collected for knockdown efficiency detection. Compared with control groups, the mRNA level of *cdc23* in siRNA- injected oocytes was significantly reduced, as examined by quantitative real-time PCR (Supplementary information, Figure S1A). As shown in Figure 2, deletion of Cdc23 with siRNA treatment apparently led to the mouse oocyte meiotic failure by exhibiting the first polar body extrusion (Figure 2A). The quantification analysis showed that the Cdc23 siRNA-injected oocytes went through the GVBD stage, without significant difference compared with the control (84.67 ± 2.404, n = 3 vs 87.67 ± 1.453, n = 3, $P > .05$, Figure 2B). However, they hardly completed first meiosis. The extrusion of PB1 in the Cdc23 siRNA-injected oocytes at 13 hours was considerably lower than that in the control group (multiple *t* tests, 41.56 ± 4.422, n = 3 vs 94.52 ± 0.6007, n = 3, $P < .001$, Figure 2C).

3.3 | Loss of Cdc23 causes spindle abnormality, chromosome misalignment, and aneuploidy

Given that Cdc23 colocalizes with spindles at MI and MII stages, we, therefore, depleted Cdc23 in oocytes and stained MI oocytes with an alpha-tubulin antibody and DAPI. We measured the MI plate width and found that it was wider in Cdc23-depleted oocytes compared to the control group. At the metaphase I stage the bivalents were aligned along the

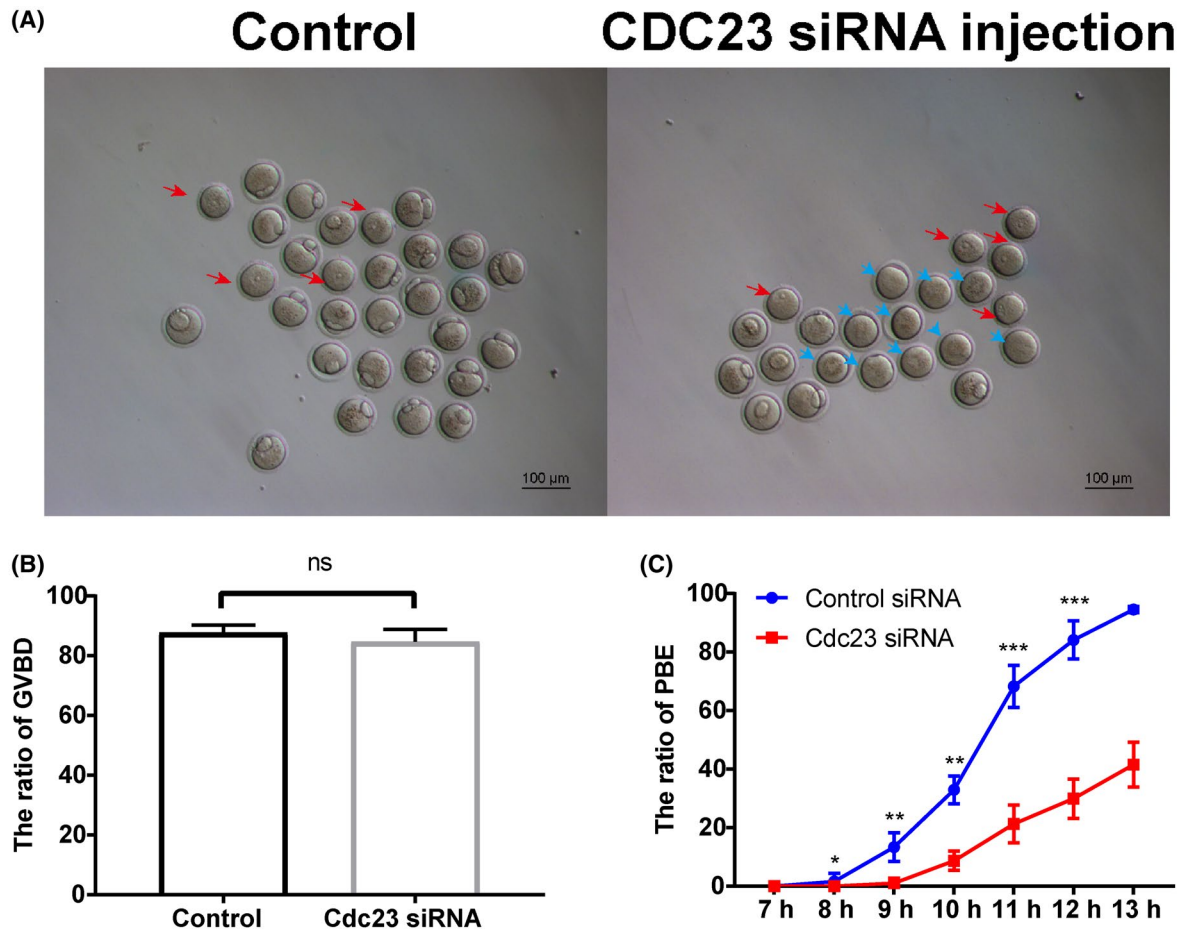

FIGURE 2 Depletion of Cdc23 impairs the first polar body extrusion in mouse oocytes. A, Representative images of control and Cdc23 knockdown oocytes cultured in vitro for 14 hours. Red arrow represents oocyte at GV stage. Blue arrow represents oocytes that did not extrude polar body. Scale bar = 100 μm. B, The rates of germinal vesicle breakdown (GVBD) were recorded in control and Cdc23 siRNA-treated oocytes (84.67 ± 2.404 vs 87.67 ± 1.453, n = 3, $P > .05$, *t* test). C, The rates of polar body extrusion were recorded in control and Cdc23 knockdown oocytes. (n = 3, *$P < .05$ **$P < .01$, ***$P < .001$, multiple *t* test)

equator in control oocytes, but were distributed disorderly in Cdc23 siRNA-injected oocytes (Figure 3A). The MI plate width was significantly increased in Cdc23 siRNA-injected oocytes compared with the control (Figure 3B). Likewise, we found that the ratio of abnormal spindles was significantly increased in Cdc23 siRNA-microinjected stage oocytes (Figure 3C,D). Chromosome spread assay of oocytes cultured for 11 hours confirmed that the homologous chromosome segregation did not occur after Cdc23 knockdown, while in the control oocytes, homologous chromosomes were separated (Figure 3E). The ratio of tetrads was analyzed and Cdc23 siRNA injected group showed a significantly higher ratio than the control group (Figure 3F). To determine whether the misaligned chromosomes and abnormal spindles in siCdc23 oocytes may generate oocytes with aneuploidy, we conducted chromosome spreading assay in MII oocytes to examine the karyotype. We found that the siCdc23 group displayed a higher aneuploidy rate compared to the control group (Figure 3G,H), providing convincing evidence for aneuploidy induction. Taken together, these findings demonstrate that loss of Cdc23 could lead to non-segregation of homologous chromosomes and failure of oocyte maturation or production of aneuploid oocytes.

3.4 | Loss of Cdc23 impairs CyclinB1 and Securin degradation

We next investigated the degradation of Cyclin B1 and securin after Cdc23 knockdown. After 24 hours siRNA treatment, oocytes were cultured in IBMX-free M16 medium. Two hours later, oocytes that went through GVBD were selected for further culture. Eight hours after GVBD, oocytes were collected. Western blot analysis showed that Cdc23 was effectively deleted by siRNA, and the expression levels of Cyclin B1 and Securin were significantly higher in the Cdc23 knockdown group compared to the control group (Figure 4A-D). To further trace the dynamic expression of Cyclin B1 during meiosis progression, we injected

Ccnb1-EGFP mRNA into GV oocyte cytoplasm. The green fluorescence remained at a high level in Cdc23 knockdown oocytes during meiosis I progression, while it declined significantly in the control oocytes with the PB1 extrusion process (Figure 5A,B). Taken together, these data suggest that Cdc23 is required for the degradation of Cyclin B1 and securin during oocyte meiosis I.

3.5 | Loss of Cdc23 prolongs MI stage with activated SAC

Having found that PB1 extrusion rate was reduced in siCdc23 oocytes, we speculated that the prolonged MI stage in Cdc23 oocytes was caused by activated SAC. To test our speculation, we detected SAC components BUB3 and MAD1 localization at 8 hours after GVBD. As expected, BUB3 was still localized at the kinetochores of the chromosomes in siCdc23 oocytes, while almost invisible in that control group. The relative fluorescence intensity of BUB3 was shown in the right panel (1.069 ± 0.05537 vs 0.0332 ± 0.007425, $n = 10$, $P < .001$, t test). (Figure 6A). Likewise, MAD1 also showed a strong localization in siCdc23 oocytes, while in the control group, Bub3 signal was weak. The relative fluorescence intensity of MAD1 was shown in the right panel (1.088 ± 0.06546 vs 0.0572 ± 0.01413, $n = 10$, $P < .001$, t test). (Figure 6B). These results demonstrate that the normal SAC inactivation was inhibited or delayed after Cdc23 deletion.

3.6 | Inhibition of Mps1 rescued the polar body extrusion in Cdc23 knockdown oocytes

Due to the sustained SAC activity in Cdc23 knockdown oocytes, we proceeded to inhibit Mps1 to test whether the inhibition of SAC could rescue the phenotype. Previous study has identified AZ3146 as a potent and selective inhibitor of Mps1.[24] Compared to the method of Mps1 siRNA microinjection, AZ3146 treatment is more optimal in compromising the function of Mps1. Oocytes were incubated in M16 media containing 2 μM AZ3146 after Cdc23 knockdown. As shown in Figure 7A, AZ3146-treated oocytes successfully extruded the first polar body, and the ratio of PBE was significantly increased after AZ3146 treatment (Figure 7B).

Having shown that Mps1 inhibition in Cdc23 knockdown oocytes accelerated the polar body extrusion in a rate similar to that observed in control oocytes, we collected oocytes at 8 hours after GVBD to test whether Mps1 inhibition can also recapitulate the decrease of securin in Cdc23 knockdown oocytes. The western blot data show that siCdc23-injected oocytes treated with Mps1-inhibitor AZ3146 do indeed have a reduction in the expression level of securin (Figure 7C,D). Thus, manipulating the SAC activity is sufficient to mimic the effect of Cdc23 deletion on the level of securin in oocytes.

4 | DISCUSSION

The findings presented here demonstrate a role of Cdc23 in the progression of mouse oocyte meiotic maturation. Our study has shown that Cdc23 locates to the spindle region and has an intense signal at the spindle poles, and it functions as an important regulator of meiotic spindle assembly and chromosome segregation. Knocking down of Cdc23 causes a reduced polar body extrusion ratio by causing aberrant spindle and SAC activation, and subsequent failed Cyclin B1 and securin degradation during first oocyte meiosis, and production of aneuploid MII oocytes.

In our study, Cdc23 shows different characteristics in mouse meiotic oocytes compared to previous studies. Cdc23 was reported to be an essential DNA replication protein playing a role in the initiation of DNA replication.[20,21] Cdc23 was reported to localize to the mitotic nucleus and to move on to the spindle in the anaphase mitotic cells.[25] Some studies reported that the localization pattern of Cdc23 resembled kinetochore components.[25-27] However, due to the technical limitations, the authors cannot rule out the possibility that the nuclear spot localization of Cdc23 actually represents the microtubule ends. Combining this information with our observation, we speculate that cdc23 may function in spindle organization due to its broad distribution on the meiotic spindle (Figure 1C).

To examine the effects of Cdc23 knockdown on spindle morphology and chromosome behavior, we analyzed the MI plate width and abnormal spindle ratio in MI stage oocytes. To synchronize the periods, we collected GV oocytes in M2 medium containing IBMX, and released them into IBMX-free M2 medium after washed for three times. After cultured for 8 hours, oocytes were collected for fixation and immunofluorescent staining. In control oocytes, the spindle morphology and chromosome alignment were significantly perturbed (Figure 3A-D). Besides, Cdc23 knockdown resulted in increased ratio of tetrads in oocytes cultured for 11 hours (Figure 3E,F). Furthermore, due to the limited number of MII oocytes, we performed chi-square test to analyze the aneuploidy ratio. Compared with control group, Cdc23 knockdown oocytes showed higher aneuploidy ratio (Figure 3G,H). The subcellular localization of CDC23 is localized to a domain that distributed in a extended region of the spindle and formed prominent spherical protrusions at MI stage, which is similar to the newly discovered class of proteins the liquid-like meiotic spindle domain (LISD),[28] we thus speculate that the underlying mechanism of CDC23 may be related to LISD proteins.[28] However, the exact mechanism

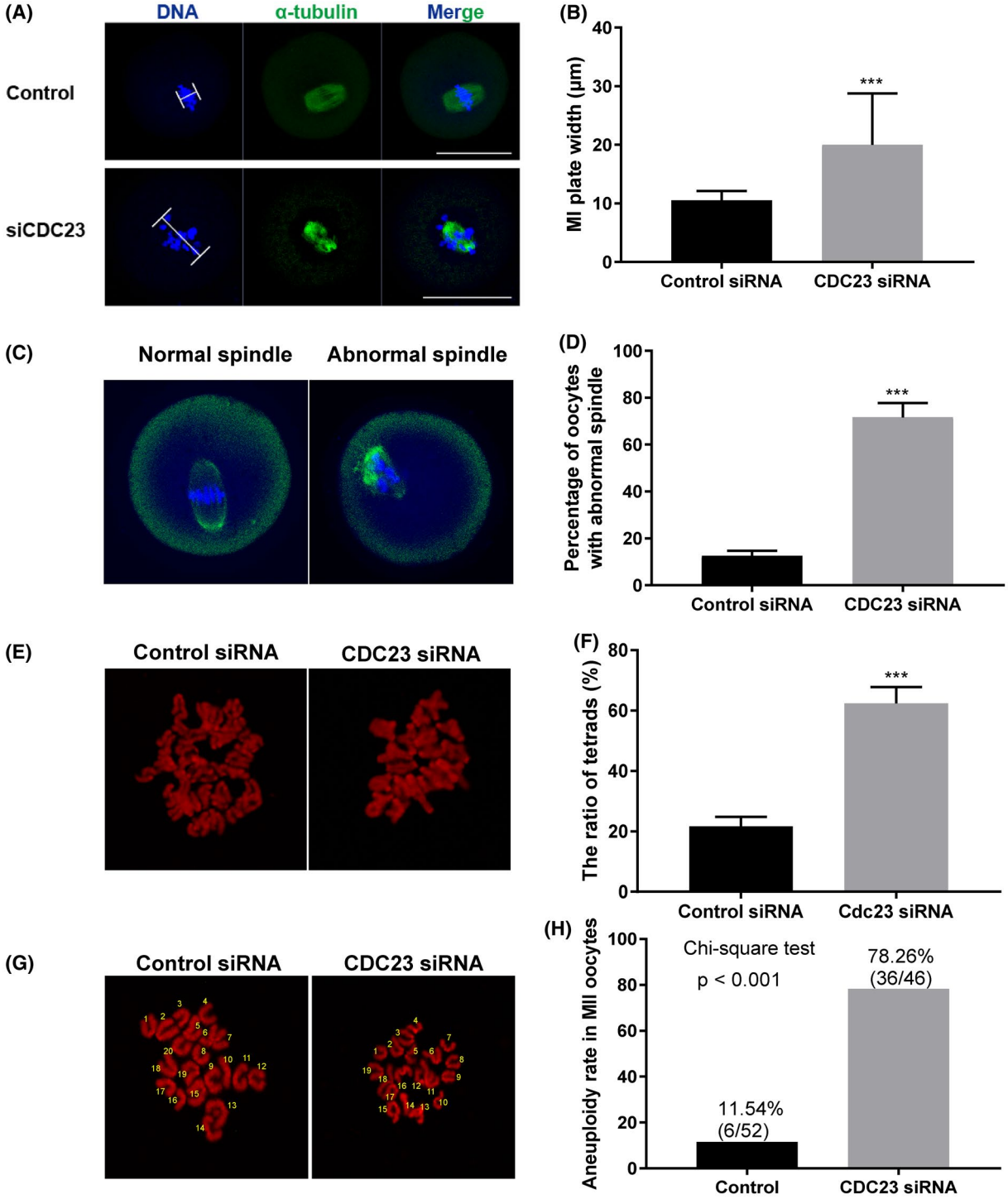

FIGURE 3 Depletion of Cdc23 increases abnormal spindles, misaligned chromosomes, non-segregation of homologous chromosomes, and aneuploidy in mouse oocytes. A, Representative images of chromosome alignment in control and Cdc23 knockdown oocytes. Oocytes were immunostained with anti-α-tubulin-F488 fluorescent antibody to visualize the spindles, and were counterstained with Hoechst 33342 to visualize the chromosomes. Scale bar = 50 μm. B, Statistical data of MI plate width in control and Cdc23 siRNA injected oocytes after cultured for 8 hours in M16 medium (10.51 ± 0.3527 vs 20.01 ± 1.914 μm, n = 21, $P < .001$, *t* test). C, Representative images of normal and abnormal spindle in MI stage oocytes. D, The rate of aberrant spindles was recorded in control and Cdc23 knockdown oocytes (81.2 ± 1.576% vs 17.71 ± 2.271%, n = 3, $P < .001$, *t* test). E, Representative chromosome spreading images of oocytes cultured for 11 hours in control and Cdc23 siRNA injected group. F, The ratio of tetrads in oocytes cultured for 11 hours after siRNA treatment (62.4 ± 3.152% vs 21.73 ± 1.81%, n = 3, $P < .001$, *t* test). G, Representative chromosome spreading images of MII oocytes in control and Cdc23 siRNA injected oocytes. H, The rate of aneuploidy was recorded in control and Cdc23-deleted MII oocytes. (Control 11.54% (6/52) vs siCDC23 78.26% (36/46), $P < .001$, Chi-square analysis). Data in B, D,F were presented as mean percentage (mean ± SEM) of at least three independent experiments. Due to the low polar body extrusion rate in siCdc23 oocytes, the aneuploidy rate was analyzed using the total number of MII oocyte in each group. The n value in H was shown above the bar plot

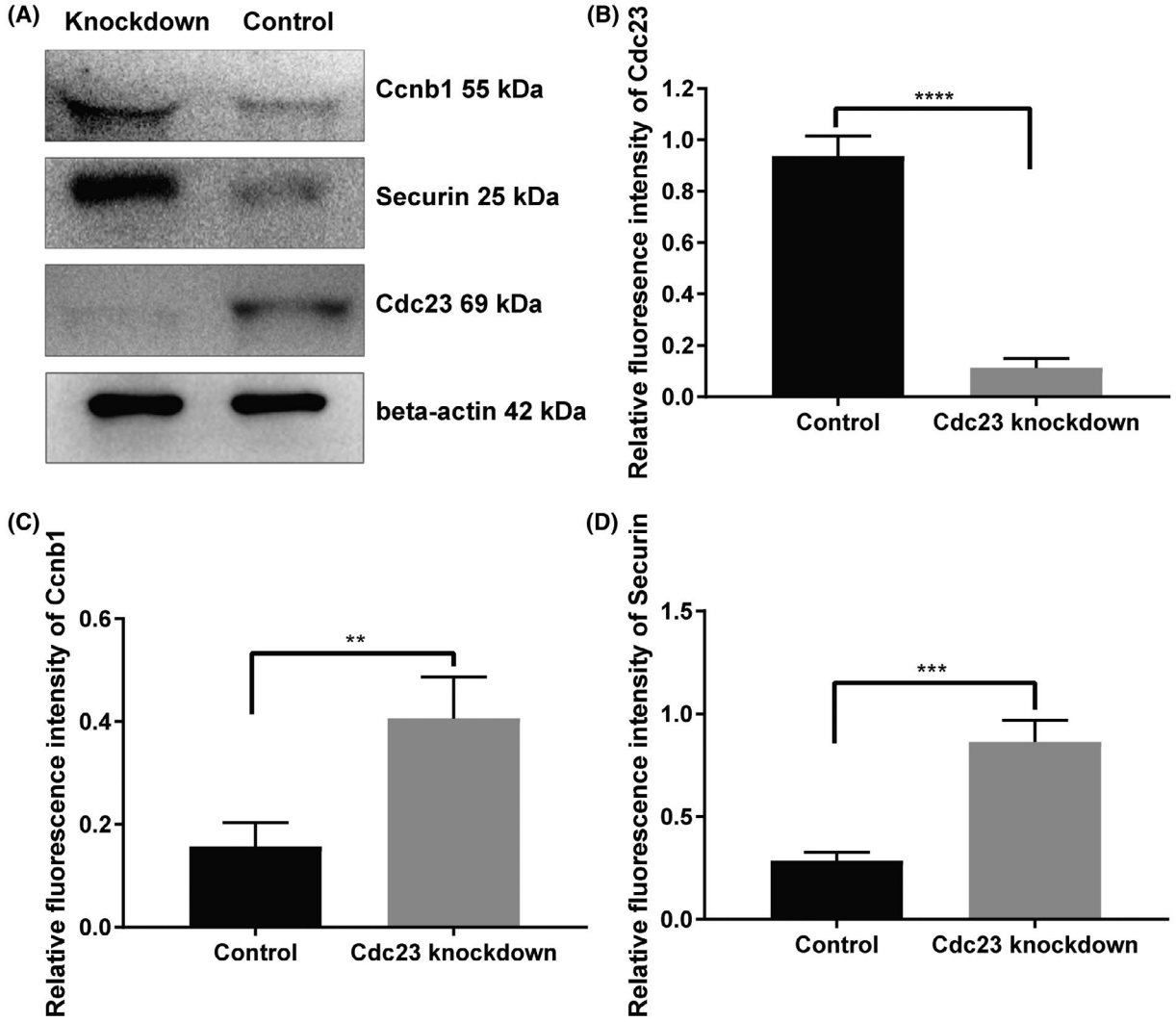

FIGURE 4 Cdc23 knockdown causes increase of cyclin B1 and securin level in mouse oocytes. A, Western blot images of control and Cdc23 knockdown oocytes 8 hours after GVBD. B, The Cdc23 siRNA effectively decreased the expression of Cdc23 (Con 0.9367 ± 0.04485 vs siCdc23 0.1133 ± 0.02028, n = 3, $P < .001$, *t* test). C, Higher cyclin B1 level in Cdc23 knockdown oocytes (0.1558 ± 0.02542, n = 3 vs 0.4076 ± 0.04456, n = 3, $P < .01$, *t* test). D, Higher securin level in Cdc23 knockdown oocytes (0.2867 ± 0.02333 vs 0.8633 ± 0.06119, n = 3, $P < .001$, *t* test)

remains unclear. Overall, the above results suggest that Cdc23 plays a critical role in spindle organization and chromosome alignment.

Due to the severely affected spindle morphology and chromosome alignment in Cdc23 knockdown oocytes, the homologous chromosomes failed to separate in time, therefore, leading to the failure of first polar body emission. Classic theory presumes that the degradation of cyclin B1 at the metaphase I to anaphase I transition is caused by APC/C-Cdc20 activation, which leads to a rapid decline in CDK1 activity, causing the exit of metaphase. As an inhibitory chaperone of separase, securin is involved in the process of the metaphase-anaphase transition regulation. The destruction of securin promotes separase cleavage of cohesin complexes, which allows homologous chromosome separation. Previous studies reported the endogenous expression level of securin and cyclin B1 during meiotic maturation, and both were significantly degraded at 8 hours after GV oocyte were released from milrinone.[5,29] Overexpression or stable expression of cyclin B1 level in oocytes during meiotic maturation delays polar body formation, suggesting that cyclin B1 needs to be efficiently degraded in oocytes for meiosis progression.[30,31] Degradation of securin is also required for separation of homologs, and non-degradable securin prevents the first PB extrusion and homolog disjunction.[32] We find that Cdc23 knockdown oocytes have an increased level of cyclin B1 and securin compared to control oocytes 8 hours after GVBD, providing solid evidence that these oocytes are arrested at the metaphase I stage. Taken together, we propose that the defect of Cdc23 caused an impaired degradation of cyclin B1 and that this aberrant accumulation of Cyclin B1 and securin leads to failure of MI-to-MII transition and first polar body extrusion.

Spindle assembly checkpoint (SAC) proteins play essential roles in both mitosis and meiosis. In mouse oocyte,

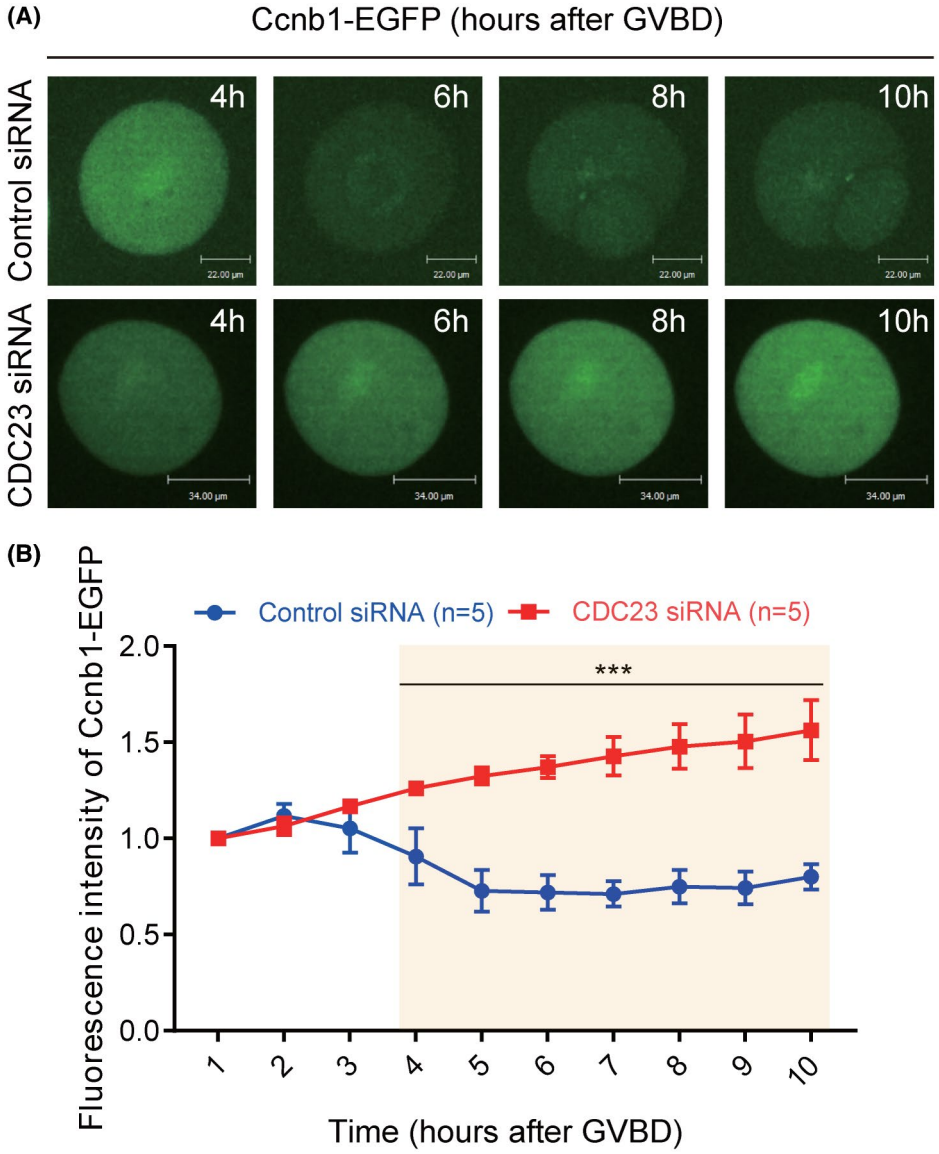

FIGURE 5 Time-lapse fluorescent imaging of Ccnb1- EGFP. A, Time-lapse fluorescent imaging of Ccnb1- EGFP 4-10 hours after GVBD. B, The fluorescent intensity of Ccnb1-EGFP were measured, background subtracted, and normalized to the initial-intensity value of GVBD oocytes. GV stage oocytes were microinjected with 10 pL 20 ng/μL Ccnb1-EGFP mRNA, incubated in M2 medium containing IBMX for 2-3 hours, and oocytes were transferred to IBMX-free M16 medium to resume meiosis. Error bars represent mean ± SEM. ***$P < .001$ (Student's *t* test)

the SAC involves the MAD (mitotic arrest deficient) proteins MPS1, MAD1, MAD2, BUBR1 (MAD3), BUB1, and BUB3.[33-37] SAC is activated when chromosomes are not properly attached to kinetochores. The activation of SAC inhibits APC/C activity through the accumulation of SAC proteins at kinetochores. The absence of SAC proteins affects meiotic division of oocytes, resulting in impaired sister chromosome separation and decreased oocyte developmental potential.[38] Previous studies by us and others reported that Mad1 may act as a negative sensor for tension or microtubule attachment. Once spindle disruption occurs, Mad1 relocates to the kinetochores.[37] During meiosis, loss of Mad1 caused misaligned chromosomes and accelerated entry into anaphase I.[36,39] The role of Bub3 in mouse oocytes has also been well-studied in our previous study. Bub3 is required for microtubule-kinetochore attachment during meiosis. Loss of Bub3 in mouse oocyte causes chromosome misalignment and abnormal polar body extrusion.[34] In our study, Bub3 and Mad1 signals were detected on kinetochores 8 hours after GVBD in Cdc23 knockdown oocytes, suggesting that the MI arrest in the Cdc23 knockdown group was due to the sustained SAC activity caused by abnormal spindle morphology and misaligned chromosomes.

Once SAC is inactivated, Cdc20 is released from MCC and binds to APC/C to initiate cyclin B1 and securin ubiquitination and degradation. To further determine the role of

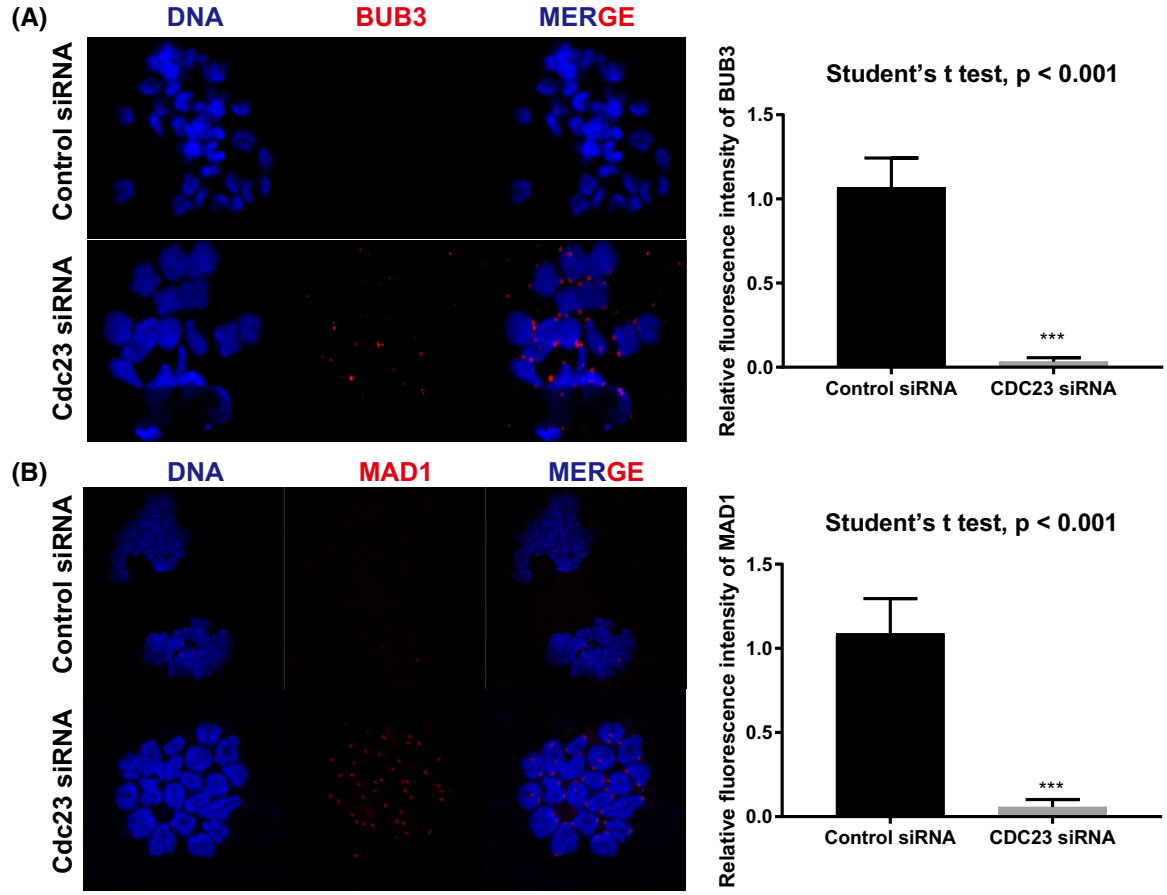

FIGURE 6 Cdc23 knockdown causes sustained activation of SAC in MI-arrested oocytes. After Cdc23 siRNA or control siRNA injection, the oocytes were inhibited in M16 containing 200uM IBMX for 24 hours, then washed thoroughly and transferred into IBMX-free M16 medium for further culture. Chromosome spread experiment was conducted 8 hours after GVBD, and stained with Bub3 (A) or Mad1 (B) antibody. Hoechst 33 342 (blue) was used to stain chromosomes. A, Bub3 (red) was localized at the kinetochores in the Cdc23 knockdown oocytes, while dissociated from kinetochores of separating homologous chromosomes in control oocytes. Right panel shows the relative fluorescence intensity of BUB3 (1.069 ± 0.05537 vs 0.0332 ± 0.007425, n = 10, $P < .001$, *t* test). B, Mad1 (red) was activated in Cdc23 knockdown oocytes, while inactivated in the control oocytes. Right panel shows the relative fluorescence intensity of MAD1 (1.088 ± 0.06546 vs 0.0572 ± 0.01413, n = 10, $P < .001$, *t* test)

SAC in causing the accumulation of cyclin B1 and securin in knockdown oocytes, we asked whether inhibition of SAC is sufficient to rescue the effect of Cdc23 deletion. If SAC is the responsible factor, its inhibition would be predicted to lead to decreased securin expression level and increase in the ratio of first polar body extrusion in the Cdc23 knockdown group. Here we utilized AZ3146 to inhibit Mps1, and the results confirm the hypothesis that SAC is the responsible factor for the decreased polar body extrusion ratio after Cdc23 knockdown (Figure 7A-D).

It is not surprising that the deletion of Cdc23 could lead to the impaired degradation of cyclin B1 and securin, since Cdc23 is a TPR protein, which was reported to be required for cyclin B proteolysis in mitotic cells. Similar function can be found with other TPR proteins, such as Cdc16, Cdc27, and Cse1 as previous studies reported.[14,16,40,41] However, it is interesting to find that SAC is activated in Cdc23 knockdown oocytes, suggesting that Cdc23 is not merely a component of APC/C, but that it is also a regulator of kinetochore-microtubule attachment.

Although SAC is recognized as an essential mechanism for the faithful chromosome segregation, researchers also reported that multiple unaligned kinetochores and severe congression defects are tolerated at the metaphase to anaphase transition in mouse oocytes, thus contributing to aneuploidy.[42] In addition, the strength of SAC is dependent on the amount of the Mad1-C-Mad2 heterotetramer at kinetochores.[43] Therefore, we speculate that the increased ratio of aneuploidy in Cdc23 knockdown MII oocytes might be due to the failure of mechanisms correcting chromosome attachment errors and recruiting insufficient quantity of MAD2 in some oocytes with misaligned chromosomes, thus delaying instead of completely inhibiting the metaphase-to-anaphase transition, although the precise mechanism is still unclear.

In summary, our study provides evidence that Cdc23 is a critical regulator in spindle assembly and chromosome segregation during mouse oocyte meiosis, suggesting a distinct role of Cdc23 in meiotic oocytes.

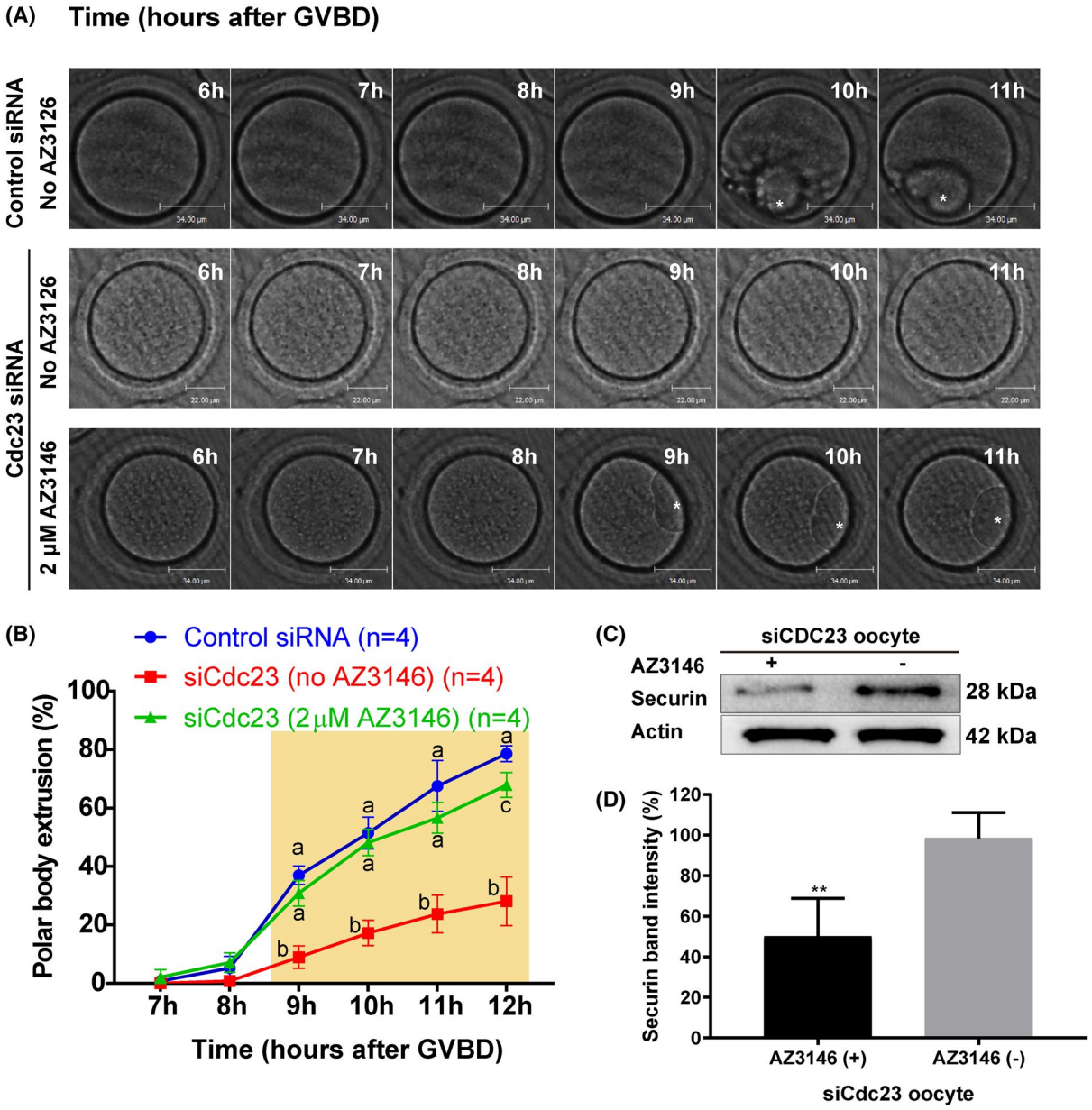

FIGURE 7 AZ3146 treatment increased polar body extrusion and reduced securin in Cdc23 knockdown oocytes. A, Time-lapse imaging of oocytes treated with AZ3146 6-11 hours after GVBD. The asterisks represent extruded polar bodies. B, The rate of polar body extrusion was recorded. At each time point, different lowercase letters represent significant difference ($P < .01$). C, Western blot image of Cdc23 knockdown oocytes treated with or without AZ3146 hours after GVBD. D, Securin band intensity was decreased in siCdc23 oocytes treated with AZ3146. (98.42 ± 7.306, n = 3 vs 49.98 ± 10.9, n = 3, $P < .01$, Student's *t* test)

ACKNOWLEDGMENTS

We appreciate and acknowledge Shiwen Li and Xili Zhu for their technical assistance. We thank Qi-Long He from Shandong Normal University for his generous technical suggestion about AZ3146.

CONFLICT OF INTEREST

The authors declare that they have no competing interests.

AUTHOR CONTRIBUTIONS

Q. Zhou designed the research; J. Li, W. Yue, A. Li, T.-G. Meng, W.-L. Lei, L.-H. Fan, and Y.-O. Ouyang helped in the experiments; Q. Zhou analyzed the data; Q. Zhou, H. Schatten, Z.-B. Wang, and Q.-Y. Sun wrote the manuscript. All authors read and approved the final manuscript.

DATA AVAILABILITY STATEMENT

All data generated or analyzed during this study are included in this published article.

REFERENCES

1. Fan H-Y, Sun Q-Y. Oocyte meiotic maturation. In: Leung P, Adashi E, eds. *The Ovary*. 3rd ed. London, United Kingdom: Academic Press; 2019:181-203.

2. Homer H. The APC/C in female mammalian meiosis I. *Reproduction*. 2013;146:R61-R71.
3. Huang JY, Morley G, Li D, Whitaker M. Cdk1 phosphorylation sites on Cdc27 are required for correct chromosomal localisation and APC/C function in syncytial Drosophila embryos. *J Cell Sci*. 2007;120:1990-1997.
4. Harper JW, Burton JL, Solomon MJ. The anaphase-promoting complex: it's not just for mitosis any more. *Genes Dev*. 2002;16:2179-2206.
5. Reis A, Madgwick S, Chang H-Y, et al. Prometaphase APCcdh1 activity prevents non-disjunction in mammalian oocytes. *Nat Cell Biol*. 2007;9:1192-1198.
6. Toda K, Naito K, Mase S, et al. APC/C-Cdh1-dependent anaphase and telophase progression during mitotic slippage. *Cell Div*. 2012;7:4.
7. Visintin R, Prinz S, Amon A. CDC20 and CDH1: a family of substrate-specific activators of APC-dependent proteolysis. *Science*. 1997;278:460-463.
8. Hagting A, den Elzen N, Vodermaier HC, et al. Human securin proteolysis is controlled by the spindle checkpoint and reveals when the APC/C switches from activation by Cdc20 to Cdh1. *J Cell Biol*. 2002;157:1125-1137.
9. Kudo NR, Anger M, Peters A, et al. Role of cleavage by separase of the Rec8 kleisin subunit of cohesin during mammalian meiosis I. *J Cell Sci*. 2009;122:2686-2698.
10. Brooker AS, Berkowitz KM. The roles of cohesins in mitosis, meiosis, and human health and disease. *Methods Mol Biol*. 2014;1170:229-266.
11. Acquaviva C, Pines J. The anaphase-promoting complex/cyclosome: APC/C. *J Cell Sci*. 2006;119:2401-2404.
12. Chang LF, Zhang Z, Yang J, McLaughlin SH, Barford D. Molecular architecture and mechanism of the anaphase-promoting complex. *Nature*. 2014;513:388-393.
13. Chang L, Zhang Z, Yang J, McLaughlin SH, Barford D. Atomic structure of the APC/C and its mechanism of protein ubiquitination. *Nature*. 2015;522:450-454.
14. Zachariae W, Nasmyth K. TPR proteins required for anaphase progression mediate ubiquitination of mitotic B-type cyclins in yeast. *Mol Biol Cell*. 1996;7:11.
15. Zhang L, Rahbari R, He M, Kebebew E. CDC23 regulates cancer cell phenotype and is overexpressed in papillary thyroid cancer. *Endocr Relat Cancer*. 2011;18:731-742.
16. Zachariae W. Mass spectrometric analysis of the anaphase-promoting complex from yeast: identification of a subunit related to cullins. *Science*. 1998;279:1216-1219.
17. Newlon CS, Fangman WL. Mitochondrial DNA synthesis in cell cycle mutants of Saccharomyces cerevisiae. *Cell*. 1975;5:423-428.
18. Lamb JR, Michaud WA, Sikorski RS, Hieter PA. Cdc16p, Cdc23p and Cdc27p form a complex essential for mitosis. *Embo J*. 1994;13:4321-4328.
19. Irniger S, Piatti S, Michaelis C, Nasmyth K. Genes involved in sister chromatid separation are needed for B-type cyclin proteolysis in budding yeast. *Cell*. 1995;81:9.
20. Gregan J, Lindner K, Brimage L, et al. Fission yeast Cdc23/Mcm10 functions after pre-replicative complex formation to promote Cdc45 chromatin binding. *Mol Biol Cell*. 2003;14:3876-3887.
21. Hart EA, Bryant JA, Moore K, Aves SJ. Fission yeast Cdc23 interactions with DNA replication initiation proteins. *Curr Genet*. 2002;41:342-348.
22. Lee J-K, Seo Y-S, Hurwitz J. The Cdc23 (Mcm10) protein is required for the phosphorylation of minichromosome maintenance complex by the Dfp1-Hsk1 kinase. *PNAS*. 2003;100:6.
23. Xu R-Y, Xu J, Wang L, et al. The Arabidopsis anaphase-promoting complex/cyclosome subunit 8 is required for male meiosis. *New Phytol*. 2019;224:229-241.
24. Hewitt L, Tighe A, Santaguida S, et al. Sustained Mps1 activity is required in mitosis to recruit O-Mad2 to the Mad1-C-Mad2 core complex. *J Cell Biol*. 2010;190:25-34.
25. Melloy PG, Holloway SL. Changes in the localization of the Saccharomyces cerevisiae anaphase-promoting complex upon microtubule depolymerization and spindle checkpoint activation. *Genetics*. 2004;167:1079-1094.
26. Zeng X, Kahana JA, Silver PA, et al. Slk19p is a centromere protein that functions to stabilize mitotic spindles. *J Cell Biol*. 1999;146:415-425.
27. Goshima G, Yanagida M. Establishing biorientation occurs with precocious separation of the sister kinetochores, but not the arms, in the early spindle of budding yeast. *Cell*. 2000;100:619-633.
28. So C, Seres KB, Steyer AM, et al. A liquid-like spindle domain promotes acentrosomal spindle assembly in mammalian oocytes. *Science*. 2019;364:eaat9557.
29. Gui L, Homer H. Hec1-dependent cyclin B2 stabilization regulates the G2-M transition and early prometaphase in mouse oocytes. *Dev Cell*. 2013;25:43-54.
30. Polanski Z, Ledan E, Brunet S, et al. Cyclin synthesis controls the progression of meiotic maturation in mouse oocytes. *Development*. 1998;125:4989-4997.
31. Ledan E, Polanski Z, Terret ME, Maro B. Meiotic maturation of the mouse oocyte requires an equilibrium between cyclin B synthesis and degradation. *Dev Biol*. 2001;232:400-413.
32. Herbert M, Levasseur M, Homer H, et al. Homologue disjunction in mouse oocytes requires proteolysis of securin and cyclin B1. *Nat Cell Biol*. 2003;5:1023-1025.
33. Sun SC, Kim NH. Spindle assembly checkpoint and its regulators in meiosis. *Hum Reprod Update*. 2012;18:60-72.
34. Li MO, Li S, Yuan JU, et al. Bub3 is a spindle assembly checkpoint protein regulating chromosome segregation during mouse oocyte meiosis. *PLoS ONE*. 2009;4:e7701.
35. Zhang D, Ma W, Li YH, et al. Intra-oocyte localization of MAD2 and its relationship with kinetochores, microtubules, and chromosomes in rat oocytes during meiosis. *Biol Reprod*. 2004;71:740-748.
36. Tunquist BJ, Eyers PA, Chen LG, Lewellyn AL, Maller JL. Spindle checkpoint proteins Mad1 and Mad2 are required for cytostatic factor-mediated metaphase arrest. *J Cell Biol*. 2003;163:1231-1242.
37. Zhang D, Li M, Ma W, et al. Localization of mitotic arrest deficient 1 (MAD1) in mouse oocytes during the first meiosis and its functions as a spindle checkpoint protein. *Biol Reprod*. 2005;72:58-68.
38. Marston AL, Wassmann K. Multiple duties for spindle assembly checkpoint kinases in meiosis. *Front Cell Dev Biol*. 2017;5:109.
39. Cheslock PS, Kemp BJ, Boumil RM, Dawson DS. The roles of MAD1, MAD2 and MAD3 in meiotic progression and the segregation of nonexchange chromosomes. *Nat Genet*. 2005;37:756-760.
40. Pal M, Nagy O, Menesi D, Udvardy A, Deak P. Structurally related TPR subunits contribute differently to the function of the

anaphase-promoting complex in Drosophila melanogaster. *J Cell Sci*. 2007;120:3238-3248.
41. Zhang Z, Roe SM, Diogon M, et al. Molecular structure of the N-terminal domain of the APC/C subunit Cdc27 reveals a homo-dimeric tetratricopeptide repeat architecture. *J Mol Biol*. 2010;397:1316-1328.
42. Sebestova J, Danylevska A, Novakova L, Kubelka M, Anger M. Lack of response to unaligned chromosomes in mammalian female gametes. *Cell Cycle*. 2012;11:3011-3018.
43. Collin P, Nashchekina O, Walker R, Pines J. The spindle assembly checkpoint works like a rheostat rather than a toggle switch. *Nat Cell Biol*. 2013;15:1378-1358.

SUPPORTING INFORMATION

Additional Supporting Information may be found online in the Supporting Information section.

How to cite this article: Zhou Q, Li J, Yue W, et al. Cell division cycle 23 is required for mouse oocyte meiotic maturation. *The FASEB Journal*. 2020;34:8990–9002. https://doi.org/10.1096/fj.202000131R